

The coordination preferences of metal centres modulate superexchange coupling interactions in a metallo-supramolecular helical assembly

Rosa Pedrido,* Miguel Vázquez López,* Lorenzo Sorace, Ana M. González- Noya, Magdalena Cwiklinska, Vanesa Suárez-Gómez, Guillermo Zaragoza and Manuel R. Bermejo

Electronic Supplementary Information (ESI)

Physical measurements and experimental techniques

Materials

All solvents, 2,6-diacetylpyridine, 4-methoxybenzylcarbazate and tetraethylammonium perchlorate are commercially available and were used without further purification. Copper and nickel metals (Ega Chemie) were used as ca. $2 \times 2 \text{ cm}^2$ plates.

Physical Measurements

Elemental analysis of C, H, N and S was performed on a FISONS EA 1108 analyzer. ^1H and ^{13}C NMR spectra were recorded on a Bruker AMX-500 spectrometer, using DMSO-d₆ as solvent. Fast atom bombardment mass spectra (FAB) were obtained on a Kratos MS-50 mass spectrometer, employing Xe atoms at 70 KeV in m-nitrobenzyl alcohol as a matrix; electrospray ionization mass spectra (ESI+) were recorded on an API4000 Applied Biosystems mass spectrometer with Triple Quadrupole analyzer. Conductivity was measured at 25 °C from 10^{-3} M solutions in DMF on a Crison micro CM 2200 conductivimeter. Magnetic measurements were performed at variable temperatures (2–300 K) and variable applied magnetic field (0–6 T) using a Cryogenic S600 SQUID magnetometer. Raw data were corrected for the sample holder contribution, measured in the same temperature range, and the intrinsic diamagnetism of the samples, estimated by Pascal's constant.

Synthesis of H₂L

H₂L (Chart S1) was prepared by condensation of 4-methoxybenzylcarbazate (0.57 g, 4.8 mmol) with 2,6-diacetylpyridine (0.46 mL, 4.8 mmol) in ethanol (150 cm³). The solution was heated under reflux for 5 h, concentrated with a Dean-Stark trap to ca. 30 cm³ and cooled for 12 h (4 °C). The white precipitate was filtered off, washed with diethyl ether (3 × 10 mL) and dried *in vacuo*.

H₂L: Yield 85%; m.p. = 200–201 °C; E.A. (Found: C, 62.2; H, 5.7; N, 13.4; C₂₇H₂₉N₅O₆ required: C, 62.0; H, 5.6; N, 13.5); FAB base peak: 520.2 amu (H₂L + H, 100%); IR (KBr, cm⁻¹): ν(NH) 3243, 3158, ν(Amide I) 1711, ν(C=N)+ν(C-N) 1613, ν(Amide II) 1569, ν(N-N) 1032; ¹H NMR (DMSO-d₆, ppm): 10.41 (s, 2H); 7.95 (d, 2H, J = 7.2 Hz), 7.84 (t, 1H, J = 7.2 Hz); 7.38 (d, 4H, J = 8.5 Hz); 6.95 (d, 4H, J = 8.5 Hz); 5.14 (s, 4H); 3.75 (s, 6H); 2.32 (s, 6H). ¹³C NMR (DMSO-d₆, ppm): δ 159.1 (C=O), 153.9 (C=N), 153.0 (CN_{py}), 130.2, 129.7, 128.1, 113.8, 113.4 (C_{ar}), 54.9 (CH₂), 30.7 (CH₃O). 12.9 (CH_{3Ac}).

General procedure for preparation of the complexes

The complexes [Cu^{II}₂(L)₂] and [Ni^{II}₂(L)₂] were synthesized by an electrochemical method¹ improved by us.² The general procedure can be typified as follows:

An acetonitrile solution of the ligand H₂L containing *ca.* 10 mg of tetraethylammonium perchlorate, as supporting electrolyte, was electrolyzed using a platinum wire as the cathode and a metal plate as the anode. The cell can be summarized as: Pt(-)|H₂L + CH₃CN|M(+), where M = Ni, Cu. (*Caution! Although problems were not encountered in our experiments, all perchlorate compounds are potentially explosive, and should be handled in small quantities and with great care*). The resulting solids were filtered off, washed with diethyl ether and dried *in vacuo*.

[Cu^{II}₂(L)₂]: Yield 89%; m.p.>300 °C; E.A. (Found: C, 55.7; H, 4.7; N, 11.9; C₅₄Cu₂H₅₄N₁₀O₁₂ required: C, 55.8; H, 4.7; N, 12.0); ESI-MS (m/z) 581.3 [CuL]⁺; 1163.3, [Cu₂L₂ + H]⁺; IR (KBr, cm⁻¹): ν(Amide I)+ν(C=N) 1715, ν(Amide II) 1514, ν(N-N) 1031; Λ_M = 5.2 μS cm⁻¹. Slow evaporation of an acetonitrile solution of the precipitated obtained yielded brown crystals of [Cu^{II}₂(L)₂]·2H₂O (**1**), which was characterized by X-ray diffraction.

[Ni^{II}₂(L)₂]: Yield 71%; m.p. >300 °C; E.A. (Found: C, 56.3; H, 4.8; N, 12.0; C₅₄H₅₄N₁₀Ni₂O₁₂ required: C, 56.3; H, 4.7; N, 12.1); ESI-MS (m/z) 576.2 [NiL]⁺, 1153.3 [Ni₂L₂ + H]⁺; IR (KBr, cm⁻¹): ν(Amide I)+ν(C=N) 1706, ν(Amide II) 1513, ν(N-N) 1023; Λ_M = 7.4 μS cm⁻¹. Slow evaporation of the mother liquors yielded the crystalline complex [Ni^{II}₂(L)₂] **2**, which was characterized by X-ray diffraction.

Crystal Structure Determinations

Colourless needles and prismatic crystals of **1** and **2**, respectively, were mounted on a glass fibre and used for data collection. Crystal data were collected at 293(2) K for **1** and 100(2) K for **2**, using a Smart-CCD-1000 BRUKER diffractometer. Graphite monochromated MoK(α) radiation ($\lambda = 0.71073 \text{ \AA}$) was used throughout. The data were processed with BRUKER SAINT³ and corrected for absorption using SADABS.⁴ The structure was solved by SIR-97⁵ and refined by full-matrix least-squares techniques against F^2 using SHELXL-97.⁶ Positional and anisotropic atomic displacement parameters were refined for all heteroatoms. Hydrogen atoms bonded to carbon were placed geometrically and the H₂O hydrogen atoms were initially positioned at sites determined from difference maps, but the positional parameters for all H atoms were included as fixed contributions riding on attached atoms with isotropic thermal parameters (1.2–1.5) times those of their carrier atoms. Criteria for a satisfactory complete analysis were the ratios of "rms" shift to standard deviation less than 0.001 and no significant features in the final difference maps. Molecular graphics were prepared with Viewer Lab and ORTEP.⁷ A highly disordered distribution of solvent for **2** was eliminated with SQUEEZE.⁸ A summary of the crystal data, experimental details and refinement results are listed in Table S1. Significant bond distances and angles are summarized in Table S2 while hydrogen bond interactions parameters are listed in Table S3.

CCDC 767303 and 767304 contain the supplementary crystallographic data for this paper. These data can be obtained free of charge from the Cambridge Crystallographic Data Centre via [ww.ccdc.cam.ac.uk/data_request.cif](http://www.ccdc.cam.ac.uk/data_request.cif).

Table S1. Selected bond lengths (\AA) for helicates **1** and **2**

Bond lengths (\AA)			
	1		2
C(1)-O(1)	1.44(2)	C(1)-O(1)	1.439(5)
C(2)-O(1)	1.369(14)	C(2)-O(1)	1.368(3)
C(8)-O(2)	1.470(11)	C(8)-O(2)	1.456(3)
C(11)-N(2)	1.296(11)	C(11)-N(2)	1.290(3)
C(12)-N(3)	1.356(10)	C(12)-N(3)	1.356(3)
C(16)-N(3)	1.332(11)	C(16)-N(3)	1.362(3)
C(18)-N(4)	1.291(10)	C(18)-N(4)	1.291(3)
C(19)-O(4)	1.250(10)	C(19)-O(4)	1.260(3)
C(19)-N(5)	1.340(11)	C(19)-N(5)	1.339(3)
C(19)-O(5)	1.353(10)	C(19)-O(5)	1.350(3)
C(20)-O(5)	1.466(11)	C(20)-O(5)	1.460(3)
C(24)-O(6)	1.377(13)	C(24)-O(6)	1.376(3)
C(27)-O(6)	1.404(15)	C(27)-O(6)	1.416(4)
C(28)-O(7)	1.424(13)	C(28)-O(7)	1.419(4)
C(29)-O(7)	1.362(11)	C(29)-O(7)	1.358(3)
C(35)-O(8)	1.447(10)	C(35)-O(8)	1.458(3)
C(36)-O(9)	1.267(10)	C(36)-O(9)	1.275(3)
C(36)-N(6)	1.333(11)	C(36)-N(6)	1.323(3)
C(36)-O(8)	1.337(10)	C(36)-O(8)	1.349(3)
C(38)-N(7)	1.279(10)	C(38)-N(7)	1.292(3)
C(39)-N(8)	1.340(10)	C(39)-N(8)	1.363(3)
C(43)-N(8)	1.375(11)	C(43)-N(8)	1.361(3)
C(45)-N(9)	1.274(11)	C(45)-N(9)	1.287(3)
C(54)-O(12)	1.427(14)	C(46)-O(10)	1.261(3)
N(2)-N(1)	1.389(10)	C(46)-N(10)	1.338(3)
N(2)-Cu(1)	1.930(7)	C(46)-O(11)	1.344(3)
N(3)-Cu(1)	2.184(6)	C(47)-O(11)	1.451(3)
N(4)-N(5)	1.386(9)	C(51)-O(12)	1.381(3)
N(4)-Cu(2)	1.946(7)	C(51)-C(52)	1.382(4)
N(6)-N(7)	1.372(10)	C(54)-O(12)	1.424(3)
N(7)-Cu(1)	1.971(7)	N(1)-N(2)	1.385(3)
N(8)-Cu(2)	2.228(6)	N(2)-Ni(1)	1.962(2)
N(9)-N(10)	1.35(2)	N(3)-Ni(1)	2.264(2)
N(9)-Cu(2)	1.906(8)	N(3)-Ni(2)	2.320(2)
O(4)-Cu(2)	2.128(6)	N(4)-N(5)	1.378(3)
O(9)-Cu(1)	2.204(6)	N(4)-Ni(2)	1.971(2)
O(12)-C(51)	1.367(11)	N(6)-N(7)	1.381(3)
Cu(2)-O(10)	2.04(2)	N(7)-Ni(1)	1.954(2)
Cu(1)-O(3)	2.003(6)	N(8)-Ni(2)	2.299(2)
N(1)-C(9)	1.323(9)	N(8)-Ni(1)	2.360(2)

C(9)-O(3)	1.262(9)	N(9)-N(10)	1.370(3)
C(9)-O(2)	1.349(9)	N(9)-Ni(2)	1.966(2)
N(10)-C(46)	1.338(15)	O(3)-Ni(1)	2.0381(17)
C(46)-O(10)	1.257(14)	O(4)-Ni(2)	2.0360(17)
C(46)-O(11)	1.350(14)	O(9)-Ni(1)	2.0468(18)
O(11)-C(47)	1.42(3)	O(10)-Ni(2)	2.0573(17)
<u>Cu(2)-Cu(1)</u>	<u>3.2418(17)</u>	Ni(1)-Ni(2)	3.0002(8)

Table S2. Selected bond angles ($^{\circ}$) for helicates **1** and **2**

Angles ($^{\circ}$)			
	1		2
O(3)-C(9)-O(2)	114.7(7)	O(3)-C(9)-O(2)	114.4(2)
N(1)-C(9)-O(2)	117.6(7)	N(1)-C(9)-O(2)	117.6(2)
C(11)-N(2)-N(1)	120.9(8)	C(11)-N(2)-N(1)	121.2(2)
N(3)-C(12)-C(11)	115.1(7)	N(3)-C(12)-C(11)	116.4(2)
N(3)-C(16)-C(15)	121.5(8)	N(3)-C(16)-C(15)	121.2(2)
C(18)-N(4)-N(5)	118.4(7)	C(18)-N(4)-N(5)	120.5(2)
N(5)-C(19)-O(5)	111.9(8)	N(5)-C(19)-O(5)	111.3(2)
O(4)-C(19)-N(5)	129.0(8)	O(4)-C(19)-N(5)	128.5(2)
N(9)-Cu(2)-O(10)	74.6(5)	N(9)-Ni(2)-O(10)	78.61(8)
N(9)-Cu(2)-N(8)	78.2(3)	N(9)-Ni(2)-N(8)	75.81(8)
N(4)-Cu(2)-O(4)	77.7(3)	N(8)-Ni(2)-N(3)	98.95(8)
O(4)-Cu(2)-O(10)	110.3(7)	N(4)-Ni(2)-N(3)	76.35(8)
N(9)-Cu(2)-N(4)	172.5(3)	N(4)-Ni(2)-O(4)	78.41(8)
O(9)-C(36)-O(8)	121.4(8)	O(4)-Ni(2)-O(10)	101.27(7)
O(9)-C(36)-N(6)	126.6(9)	N(9)-Ni(2)-N(4)	176.99(9)
C(38)-N(7)-N(6)	118.2(7)	O(9)-C(36)-O(8)	113.8(2)
N(8)-C(39)-C(38)	116.4(7)	O(9)-C(36)-N(6)	128.1(2)
N(8)-C(43)-C(45)	115.2(8)	C(38)-N(7)-N(6)	120.5(2)
C(45)-N(9)-N(10)	111.2(10)	N(8)-C(39)-C(38)	116.8(2)
O(10)-C(46)-N(10)	128.5(17)	N(8)-C(43)-C(45)	116.3(2)
O(10)-C(46)-O(11)	118.5(17)	C(45)-N(9)-N(10)	119.7(2)
N(7)-Cu(1)-O(3)	94.7(3)	O(10)-C(46)-N(10)	128.2(2)
N(2)-Cu(1)-N(3)	78.2(3)	O(10)-C(46)-O(11)	120.5(2)
N(2)-Cu(1)-O(3)	79.3(3)	N(7)-Ni(1)-O(3)	99.02(8)
O(3)-Cu(1)-O(9)	114.2(2)	N(7)-Ni(1)-N(8)	75.96(8)
N(7)-Cu(1)-N(2)	171.6(3)	N(2)-Ni(1)-N(3)	76.58(8)
		N(2)-Ni(1)-O(3)	78.95(8)
		O(3)-Ni(1)-O(9)	105.76(7)
		N(7)-Ni(1)-N(2)	175.37(9)
		N(3)-Ni(1)-N(8)	98.81(8)

Table S3. Hydrogen bond parameters [\AA , $^\circ$] for **1** and **2**

Parameter	D-H \cdots A	D-H	H \cdots A	D \cdots A	\angle DHA
	1				
013—H13B \cdots N6	0.81 (6)	2.18 (7)	2.971 (11)	166 (13)	
013—H13A \cdots O12 ⁱ	0.87 (8)	2.19 (8)	3.027 (11)	163 (13)	
014—H14B \cdots O13 ⁱⁱ	0.94 (8)	2.04 (9)	2.979 (14)	177 (14)	
014—H14A \cdots N5 ⁱⁱ	0.84 (14)	2.25	3.047 (12)	159 (14)	
		(14)			
C10—H10C \cdots N1	0.96	2.39	2.828 (12)	107	
C44—H44A \cdots N10	0.96	2.17	2.60(2)	106	
C20—H20B \cdots O1 ⁱⁱⁱ	0.97	2.53	3.384(12)	147	
C26—H26 \cdots O4 ^{iv}	0.93	2.58	3.323(12)	137	
C27—H27A \cdots O3 ^v	0.96	2.52	3.450(14)	162	
C42—H42 \cdots O7 ^{vi}	0.93	2.51	3.349(12)	151	
<hr/>					
<i>Symmetry transformations:</i> (i) $x+1, y+1, z$; (ii) $x-1, y, z$; (iii) $x+1, y, z$; (iv) $-x+1, -y, -z+1$;					
<hr/>					
	2				
C10—H10A \cdots N1	0.96	2.44	2.851(3)	106	
C13—H13 \cdots O9 ⁱ	0.93	2.51	3.395(3)	159	
C17—H17A \cdots N6	0.96	2.5	2.841(4)	101	
C26—H26 \cdots O4 ⁱⁱ	0.93	2.54	3.421(4)	159	
C27—H27C \cdots O ³ⁱⁱⁱ	0.96	2.39	3.299(4)	159	
C35—H35B \cdots N7	0.97	2.23	2.668(4)	106	
C37—H37A \cdots N7	0.96	2.5	2.838(4)	100	
C42—H42 \cdots O7 ^{iv}	0.93	2.37	3.264(4)	162	
<hr/>					
<i>Symmetry transformations:</i> (i) $-x+2, -y, -z+1$; (ii) $-x+2, -y+1, -z+2$; (iii) $-x+2, -y, -z+2$; (iv) $x+1, y+1, z+1$.					
<hr/>					

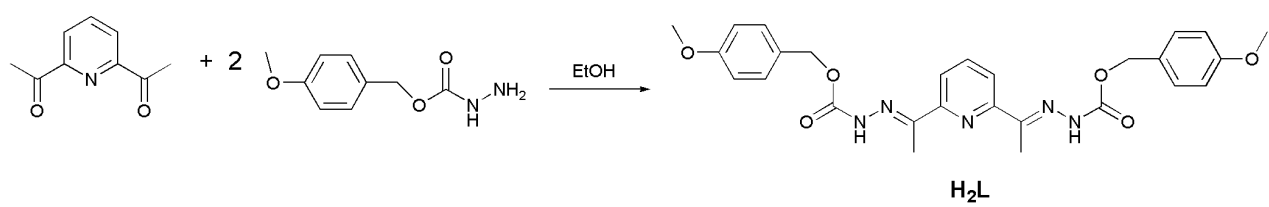


Chart S1: Synthesis of the ligand **H₂L**.

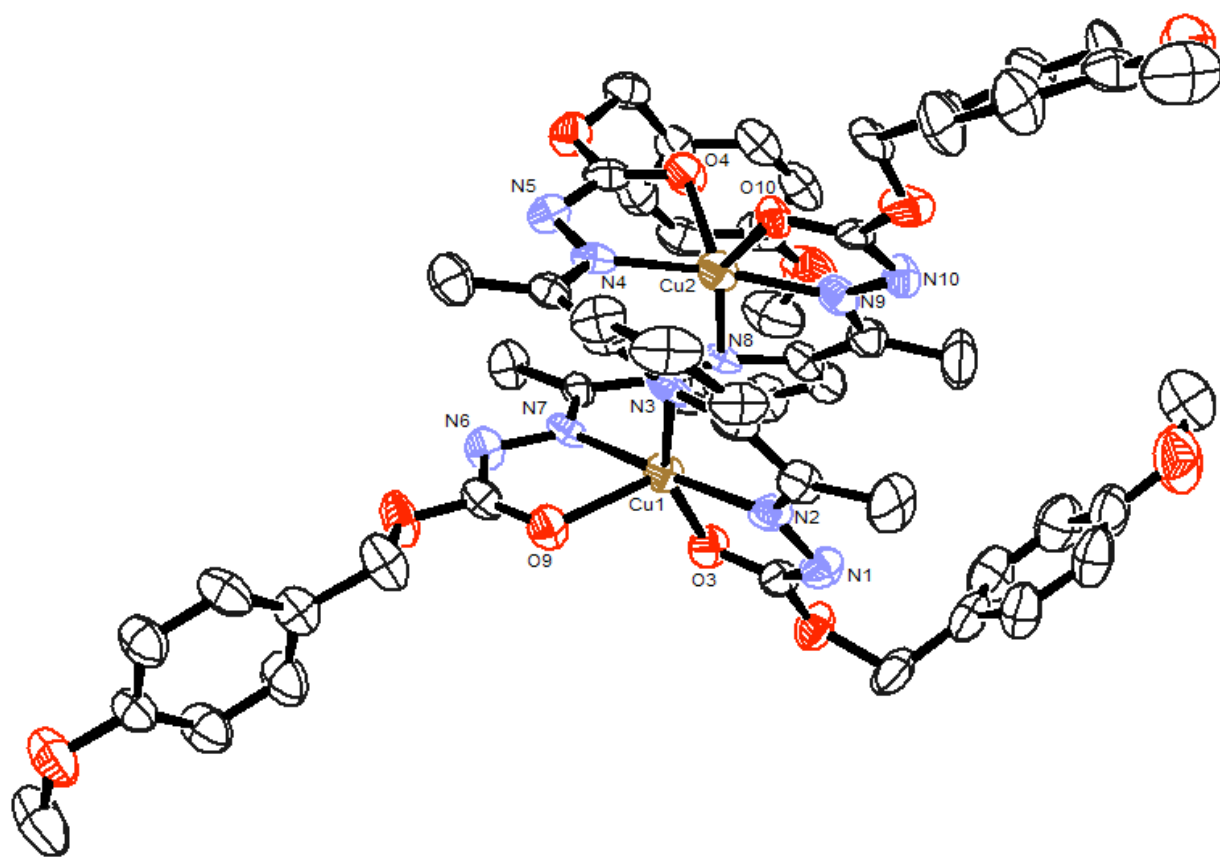


Figure S1. ORTEP diagram for the complex $[\text{Cu}^{\text{II}}_2(\text{L})_2] \cdot 2\text{H}_2\text{O}$ **1**. Solvating water molecules and disordered atoms are not depicted for the sake of clarity.

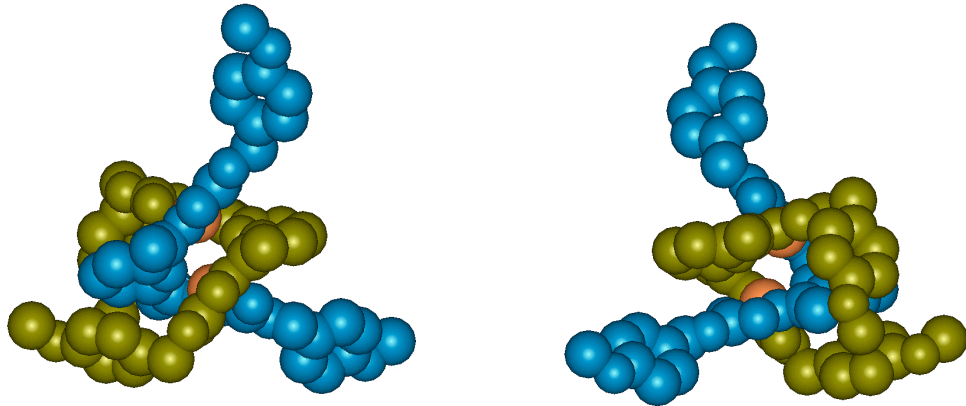


Figure S2. Major and minor grooves in the asymmetric helicate $[\text{Cu}^{\text{II}}_2(\text{L})_2]\cdot 2\text{H}_2\text{O}$ **1**.

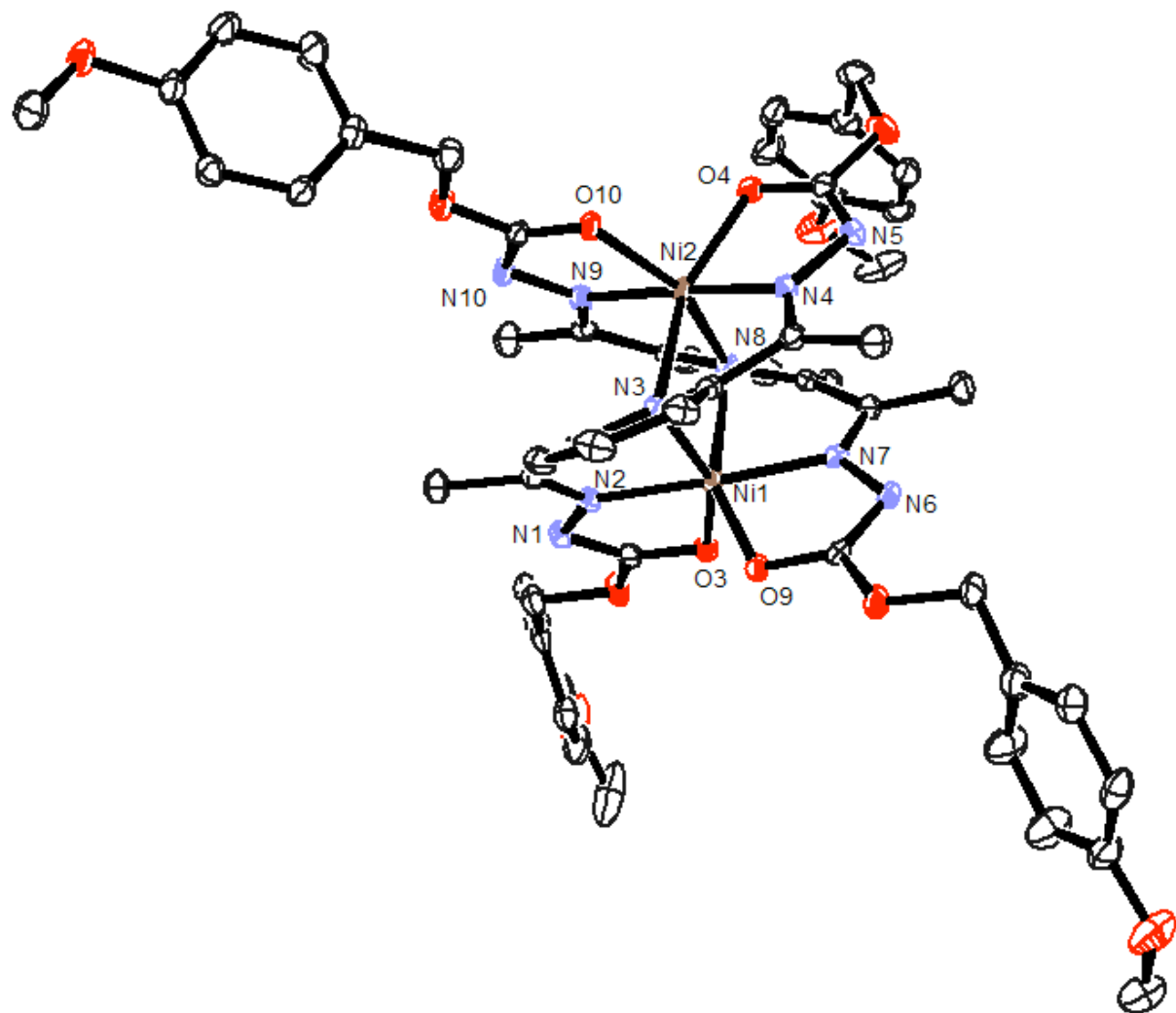


Figure S3. ORTEP diagram for the complex $[\text{Ni}^{\text{II}}_2(\mathbf{L})_2]$ (2).

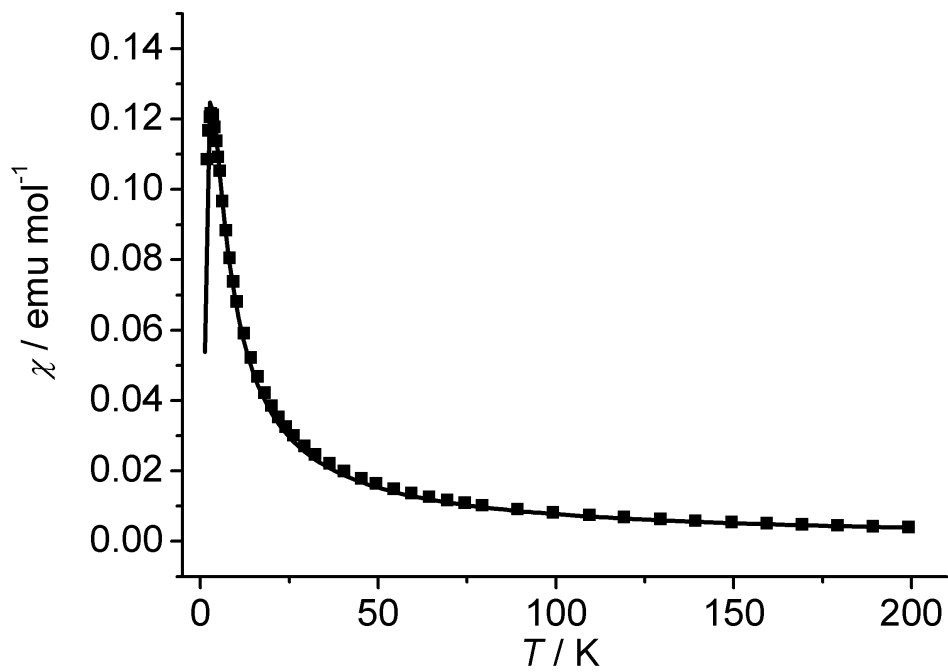


Figure S4. Plot of χ vs T curve for **1** and corresponding best fit curve obtained with parameters reported in the text.

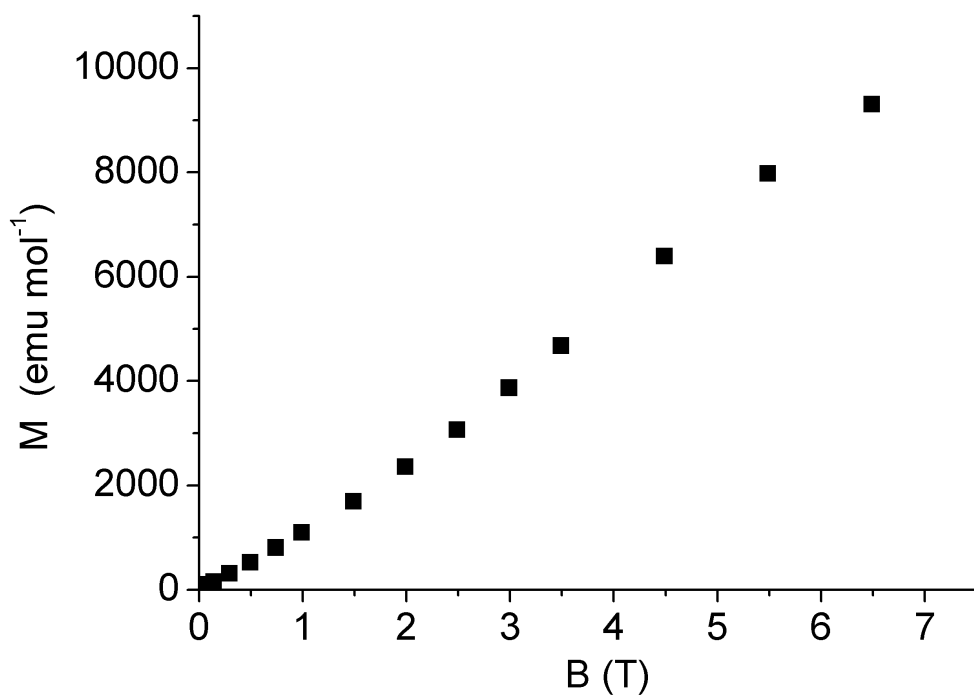


Figure S5. Field dependent magnetization curve for **1**, measured at 2 K. The inflection point around 4 T indicates the occurrence of the field induced spin state transition, from singlet to triplet.

ESI references

- (1) M. A. Khan, R. Kumar, D. G. Tuck, *Polyhedron*, 1988, **7**, 49–55.
- (2) M. Vázquez, A. Taglietti, D. Gatteschi, L. Sorace, C. Sangregorio, A. M. González, M. Maneiro, R. Pedrido, M. R. Bermejo, *Chem. Commun.*, 2003, 1840.
- (3) SAINT, *Siemens Area detector integration software*, Bruker AXS Inc., Madison, WI, USA, 2003.
- (4) G. M. Sheldrick, *SADABS, Program for Scaling and Correction of Area Detector Data*, University of Göttingen, Germany, 1996.
- (5) A. Altomare, C. Cascarano, C. Giacovazzo, A. Guagliardi, A. G. G. Moliterni, M. C. Burla, G. Polidori, M. Camalli, R. Spagna, *SIR97*. University of Bari, Italy, 1997.
- (6) G. M. Sheldrick, *Acta Crystallogr.*, 2008, **A64**, 112–122.
- (7) L. J. Farrugia, ORTEP-3 for Windows *J. Appl. Cryst.*, 1997, **30**, 565–566.
- (8) P. van der Sluis, A. L. Spek, *Acta Crystallogr. Sect. A: Found. Crystallogr.* 1990, **46**, 194–201.